

DOI: 10.1002/adma.((please add manuscript number))

## Near-Incompressible Faceted Polymer Microcapsules from Metal-Organic Framework Templates

By *Hiroataka Ejima, Nobuhiro Yanai, James P. Best, Melinda Sindoro, Steve Granick\** and *Frank Caruso\**

[\*] Prof. F. Caruso, Dr. H. Ejima, J. P. Best

Department of Chemical and Biomolecular Engineering, The University of Melbourne, Parkville, Victoria 3010 (Australia)

E-mail: fcaruso@unimelb.edu.au

Prof. S. Granick, Dr. N. Yanai, M. Sindoro

Department of Materials Science and Engineering, Department of Chemistry, and Department of Physics, University of Illinois, Urbana, Illinois 61801 (USA)

E-mail: sgranick@illinois.edu

Keywords: (polymer capsules, metal-organic framework, layer-by-layer, nanomechanics)

Spherical polymer microcapsules have been extensively studied over the last decade for applications in a wide range of fields.<sup>[1]</sup> Recently, control over microcapsule shape has attracted much interest; however, studies on faceted polymer microcapsules have been limited to only tetrahedral<sup>[2]</sup> and hexahedral<sup>[2-3]</sup> geometries, due to the challenge of finding appropriate template materials. Herein, we exploit for the first time metal-organic framework (MOF) crystals as templates to prepare monodisperse rhombic dodecahedral microcapsules. The MOF crystals can be completely removed under mild aqueous conditions, thus providing an advantageous class of template material for microcapsule preparation. The obtained faceted microcapsules are stiffer than spherical counterparts of the same size and shell thickness, reflecting the near-incompressibility of the facet edges. During observation of up to one month, there is no tendency for these hollow polyhedra to revert toward a lower-energy spherical geometry. These results suggest that faceting can be used as a powerful strategy for tuning the mechanical properties of polymer microcapsules.

Faceted geometries are widely found in naturally occurring particles (*e.g.*, viruses), and play a pivotal role in material properties such as elasticity and stiffness.<sup>[4]</sup> Polymer

microcapsules with a spherical shape have often been prepared via the layer-by-layer (LbL) method<sup>[5]</sup> for potential applications in drug/gene delivery, catalysis, biosensing, and microreactors.<sup>[1]</sup> Recently, control over the shape of LbL capsules has emerged as an exciting research area, as anisotropic colloids exhibit geometrically dependent interactions with biological interfaces,<sup>[6]</sup> such as in cellular processing.<sup>[7]</sup> To date, spherical (melamine formaldehyde,<sup>[5]</sup> polystyrene,<sup>[8]</sup> silica,<sup>[9]</sup> polylactic acid,<sup>[10]</sup> poly(lactic-*co*-glycolic acid),<sup>[10]</sup> calcium carbonate,<sup>[3a, 3e]</sup> manganese carbonate,<sup>[3a, 11]</sup> gold<sup>[12]</sup>), elongated (nickel,<sup>[13]</sup> glass fiber,<sup>[14]</sup> calcium carbonate,<sup>[3b, 3e]</sup> silica<sup>[7]</sup>), tetrahedral (tin sulfide<sup>[2]</sup>), and hexahedral (calcium carbonate,<sup>[3b, 3e]</sup> cadmium carbonate,<sup>[2, 3d, 3f]</sup> manganese carbonate<sup>[3c, 3d, 3g]</sup>) templates have been exploited to prepare LbL capsules, in addition to biological cellular templates.<sup>[15]</sup> Despite such advances, fundamental studies on the correlation between complex capsule shape and mechanical properties are limited.

Control over capsule shape relies on the development of novel removable template materials with diverse geometries, for use in the LbL process. MOF particles are ideal materials in this respect since they offer various shapes, in colloidal-sized form.<sup>[16]</sup> MOFs are a class of well-defined microporous materials that consist of metal nodes bridged with organic ligands. To further expand on the potential of MOFs, covalent functionalization of MOF surfaces is a vibrant area of chemistry.<sup>[17]</sup> Our non-covalent LbL approach on the surface modification of MOFs and subsequent hollow capsule formation are summarized in **Scheme 1**. In this paper, the prototypical MOF, [Zn(mim)<sub>2</sub>]<sub>n</sub> (ZIF-8; mim = 2-methylimidazolate),<sup>[18]</sup> was used due to its distinctive shape (rhombic dodecahedron; polyhedron with 12 congruent rhombic faces) and the recent discovery that such particles can be produced to be highly monodisperse<sup>[16e, 16f]</sup> with tunable size.<sup>[16g]</sup> As an assembling polymer pair, poly(4-styrene sulfonic acid) (PSS) and poly(allylamine) (PA) were chosen, as they are well-established materials for LbL assembly.<sup>[19]</sup> The advantages of PSS/PA films include: (i) their stability under a wide pH range (1 – 11);<sup>[20]</sup> (ii) tunable permeability by the number of LbL deposition

steps;<sup>[21]</sup> and (iii) surface functionalization capability with low fouling polymers<sup>[22]</sup> and antibodies<sup>[23]</sup> for targeted drug/gene delivery applications. The consecutive assembly of PSS/PA can also be performed in both aqueous solutions and organic solvents.<sup>[24]</sup> The MOF templates were removed through treatment with ethylenediaminetetraacetic acid (EDTA), and the resulting hollow capsules were characterized by scanning electron microscopy (SEM), transmission electron microscopy (TEM), atomic force microscopy (AFM), and confocal laser scanning microscopy (CLSM).

The LbL assembly was initiated with the adsorption of negatively charged PSS onto the positively charged MOF crystals (see Supporting Information). Methanol was selected as the solvent, as these MOFs are unstable in aqueous conditions, though water is the traditional solvent for LbL assembly. After the adsorption steps, non-adsorbed polymer in solution was removed via three separate centrifugation and washing cycles. The zeta ( $\zeta$ )-potential, measured in methanol, initially changed from positive ( $46.9 \pm 10.5$  mV) to negative ( $-26.5 \pm 13.9$  mV) in accordance with the adsorption of PSS. After the PA adsorption as a second layer, the  $\zeta$ -potential returned to a positive value ( $57.2 \pm 14.1$  mV). The alternating positive and negative  $\zeta$ -potential values was further observed throughout the LbL process (**Figure 1a**), indicating the successive adsorption of PSS and PA on the MOF crystal surface.

To observe the growth of LbL films, the multilayer films were assembled on a quartz crystal microbalance (QCM). Figure 1b shows the decrease in resonance frequency ( $\Delta F$ ) after each adsorption step. The growth was essentially proportional to the number of layers, as previously observed in water.<sup>[25]</sup> The  $\Delta F$  after deposition of 10 layers was  $821 \pm 4$  Hz, corresponding to *ca.* 22 nm, estimated using the Sauerbrey relation (see Supporting Information). In the case of PSS/PA assembly on MOF crystals, linear buildup was also confirmed (Supporting Information, Figure S1). This was achieved by observing the increase of fluorescence intensity with each deposition of a fluorescently labeled polymer (FITC-PA).

It is noted that the assembly was started with PA for QCM measurements, while PSS was initially adsorbed on MOF crystals due to the difference of substrate surface charge.

Figure 1c and 1d show SEM images of the MOF crystals before and after the LbL coating. The distinctive rhombic dodecahedral shape was retained after the LbL process. From TEM observations, the polymeric multilayers (*ca.* 20 nm thick) visibly coated the MOF crystals (Supporting Information, Figure S2a,b). AFM observations (Supporting Information, Figure S2c,d) revealed the facets of LbL-coated MOF crystals to be quite flat (peak-to-valley roughness of 4.4 nm over a 200 nm × 200 nm area), which is only slightly rougher than the bare surface of MOF crystals (Supporting Information, Figure S3).

MOF cores were removed in aqueous EDTA solution (0.1 M, pH 7). The attenuated total reflection Fourier transform infrared (ATR-FTIR) spectral pattern for the obtained capsules (Supporting Information, Figure S4) was nearly identical to previously reported spectra for PSS/PA complexes.<sup>[15a]</sup> No peaks attributable to the MOF templates were detected,<sup>[16f, 26]</sup> suggesting that the MOF templates were completely removed. Energy-dispersive X-ray spectroscopy (EDX) also showed no detectable Zn in the LbL shell after template removal (Supporting Information, Figure S5). **Figure 2a** and **2b** show SEM and TEM images of the capsules, respectively. Since these measurements were carried out after drying, the capsules had collapsed. Folds and creases were observed, as previously reported for spherical ((PSS/PA)<sub>4</sub>/PSS) capsules.<sup>[5]</sup> However, folds with rhombus shapes originating from the {110} MOF facets are also visible in the TEM image (Figure 2b). From AFM height profiles (Supporting Information, Figure S6), the film thickness was 20.3 ± 2.0 nm, consistent with the aforementioned QCM and TEM results. Dried capsules were likely to aggregate (Figure 2a) due to strong interactions between large and flat facets.

CLSM was also employed to visualize the capsule shape in aqueous solution (Figure 2c-e). Optical sections were collected after negatively charged capsules ((PSS/FITC-PA)<sub>4</sub>/PSS) were electrostatically adsorbed onto a polyethyleneimine (PEI)-coated cover glass.

Two-dimensional (2D) image sections (Figure 2c) show well-dispersed polymer capsules with hexagonal shape. Unlike cases for mesoporous materials,<sup>[27]</sup> infiltration of polymer into pores of the MOF crystals did not occur during the LbL process (Figure 2c-e), as the MOF pore size used in this study is 1.16 nm connected through narrow windows of 0.34 nm,<sup>[18]</sup> considerably smaller than the hydrodynamic radius ( $R_h$ ) of the employed polymers.<sup>[28]</sup> A set of 2D cross-sectional images in the x-y plane, along the z-axis, was collected to reconstruct a three-dimensional (3D) image of a single capsule (Figure 2d). Slice images at a z-axis interval of 81 nm are shown in Figure 2e. From these experiments, we conclude that the rhombic dodecahedral geometry of the MOF template was retained in aqueous solution even after core removal. The capsules are stable in the broad pH range (1–11), and retain their shape in water for at least one month.

The mechanical properties of the rhombic dodecahedral capsules in water were compared to those of spherical capsules of the same size. It is noted that the shell thickness of spherical capsules used ( $20.8 \pm 1.5$  nm) were within experimental error of those observed for rhombic dodecahedral capsules. **Figure 3a** shows representative force-deformation curves for both systems. In these experiments, a cantilever modified with a large colloidal probe (diameter *ca.* 30  $\mu\text{m}$ ) was used to apply a force to capsules immobilized on a PEI-coated glass substrate. For the cantilever used, the average system stiffness was determined as  $292 \pm 73$  and  $76 \pm 21$   $\text{mN m}^{-1}$  for dodecahedral and spherical capsules, respectively. Generally, however, it was found that the rhombic dodecahedral capsules demonstrated near incompressible behavior at low applied forces, until a ‘buckling’ transition point<sup>[29]</sup> is reached (*ca.* 6 nN), as shown in Figure 3a. While the molecular origins are necessarily speculative based on just an AFM compression test, it is notable that near incompressibility was predicted theoretically by Vaziri and coworkers,<sup>[30]</sup> who anticipated that bending of cell edges governs the ultimate bending properties for large contact area deformations. Applied to this system, it

would imply that mechanical resistance at facet edges is responsible for the enhanced stiffness observed.

Pursuing this hypothesis, we used a sharp-tipped probe to conduct a high-resolution force tomography analysis of individual dodecahedral capsules in water, as shown in Figure 3b. A force curve was collected every 100 nm over a  $5 \times 5 \mu\text{m}$  grid in order to analyze the force response over the capsule surface. It was seen that the stiffness, and Young's modulus ( $E_Y$ ), along the facet edges were of similar incompressibility to that of the substrate, while the capsule was softest at maximal distances from the facet edges, consistent with our hypothesis. Fery and coworkers investigated the mechanical properties of faceted surfactant vesicles and demonstrated that the shell is stiffer on vertexes than on the facets,<sup>[31]</sup> in agreement with our results.

Furthermore, the Reissner relationship for thin-walled spherical shells gives  $E_Y = 89.1 \pm 24.3 \text{ MPa}$  at  $26 - 28 \text{ }^\circ\text{C}$ . This value correlates well with average localized  $E_Y$  results obtained for the tomography analysis of the rhombic dodecahedral capsules using the Hertz-Sneddon relationship, under the same conditions. We expected this to be the case, as the material is consistent between the two systems. We are aware of only one earlier study of  $E_Y$  for faceted polymer microcapsules, in this case cubic polyelectrolyte capsules prepared from cadmium carbonate templates.<sup>[3d]</sup> However, only small contact area deformation was investigated, and the cubic capsules did not display the enhanced stiffness that we report here for the more complex polyhedron, as the LbL shells became softer due to the pore formation via unfavorable  $\text{CO}_2$  production during dissolution of the carbonate template.

In conclusion, hollow, faceted polymer microcapsules with 12 congruent faces were obtained through dissolution of the MOF templates coated with polymer multilayers. The microcapsules were mechanically stable, with an enhanced stiffness mediated by the strength of the facet edges. We envisage that MOF crystals will prove to be an important class of template material, with a wide variety of structures useful for LbL capsule formation possible.

### Experimental

A detailed description of experimental procedures can be found in the Supporting Information.

### Acknowledgements

The Australian Research Council is acknowledged for support under the Federation Fellowship (FF0776078), Australian Laureate Fellowship (FL120100030), and Discovery Project (DP0877360) schemes. This work was also supported by the US Army Research Office (grant award no. W911NF-10-1-0518). H.E. and N.Y. thank JSPS Postdoctoral Fellowships for Research Abroad.

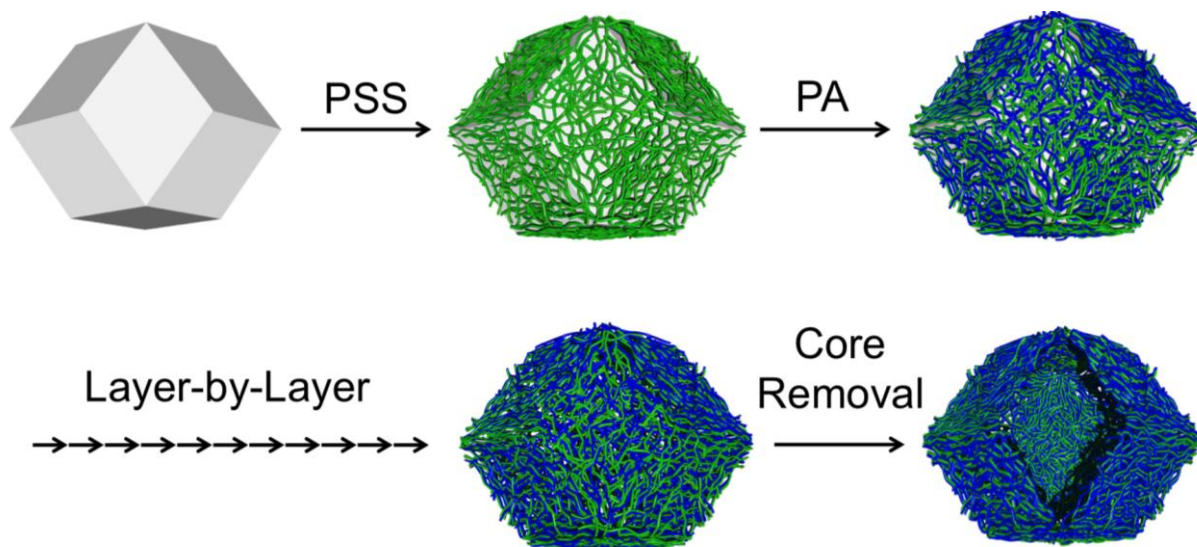
Received: ((will be filled in by the editorial staff))

Revised: ((will be filled in by the editorial staff))

Published online: ((will be filled in by the editorial staff))

- [1] a) C. S. Peyratout, L. Dahne, *Angew. Chem., Int. Ed.* **2004**, *43*, 3762; b) K. Ariga, J. P. Hill, Q. M. Ji, *Phys. Chem. Chem. Phys.* **2007**, *9*, 2319; c) G. D. Fu, G. L. Li, K. G. Neoh, E. T. Kang, *Prog. Polym. Sci.* **2011**, *36*, 127; d) G. K. Such, A. P. R. Johnston, F. Caruso, *Chem. Soc. Rev.* **2011**, *40*, 19; e) S. De Koker, R. Hoogenboom, B. G. De Geest, *Chem. Soc. Rev.* **2012**, *41*, 2867; f) B. M. Wohl, J. F. J. Engbersen, *J. Controlled Release* **2012**, *158*, 2.
- [2] O. Shchepelina, V. Kozlovskaya, E. Kharlampieva, W. B. Mao, A. Alexeev, V. V. Tsukruk, *Macromol. Rapid Commun.* **2010**, *31*, 2041.
- [3] a) A. A. Antipov, D. Shchukin, Y. Fedutik, A. I. Petrov, G. B. Sukhorukov, H. Möhwald, *Colloids Surf., A* **2003**, *224*, 175; b) B. Holt, R. Lam, F. C. Meldrum, S. D. Stoyanov, V. N. Paunov, *Soft Matter* **2007**, *3*, 188; c) V. Kozlovskaya, W. Higgins, J. Chen, E. Kharlampieva, *Chem. Commun.* **2011**, *47*, 8352; d) O. Shchepelina, M. O. Lisunova, I. Drachuk, V. V. Tsukruk, *Chem. Mater.* **2012**, *24*, 1245; e) A. Yashchenok, B. Parakhonskiy, S. Donatan, D. Kohler, A. Skirtach, H. Möhwald, *J. Mater. Chem. B* **2013**, *1*, 1223. f) V. Kozlovskaya, S. Yakovlev, M. Libera, S. A. Sukhishvili, *Macromolecules* **2005**, *38*, 4828; g) V. Kozlovskaya, Y. Wang, W. Higgins, J. Chen, Y. Chen, E. Kharlampieva, *Soft Matter* **2012**, *8*, 9828.
- [4] W. H. Roos, I. L. Ivanovska, A. Evilevitch, G. J. L. Wuite, *Cell. Mol. Life Sci.* **2007**, *64*, 1484.
- [5] E. Donath, G. B. Sukhorukov, F. Caruso, S. A. Davis, H. Möhwald, *Angew. Chem., Int. Ed.* **1998**, *37*, 2202.
- [6] J. P. Best, Y. Yan, F. Caruso, *Adv. Healthcare Mater.* **2012**, *1*, 35.
- [7] O. Shimoni, Y. Yan, Y. Wang, F. Caruso, *ACS Nano* **2013**, *7*, 522.
- [8] F. Caruso, R. A. Caruso, H. Möhwald, *Science* **1998**, *282*, 1111.
- [9] P. Schuetz, F. Caruso, *Adv. Funct. Mater.* **2003**, *13*, 929.
- [10] D. B. Shenoy, A. A. Antipov, G. B. Sukhorukov, H. Möhwald, *Biomacromolecules* **2003**, *4*, 265.
- [11] H. G. Zhu, E. W. Stein, Z. H. Lu, Y. M. Lvov, M. J. McShane, *Chem. Mater.* **2005**, *17*, 2323.
- [12] D. I. Gittins, F. Caruso, *Adv. Mater.* **2000**, *12*, 1947.
- [13] K. S. Mayya, D. I. Gittins, A. M. Dibaj, F. Caruso, *Nano Lett.* **2001**, *1*, 727.
- [14] R. Müller, L. Daehne, A. Fery, *J. Phys. Chem. B* **2007**, *111*, 8547.
- [15] a) S. Moya, L. Dahne, A. Voigt, S. Leporatti, E. Donath, H. Möhwald, *Colloids Surf., A* **2001**, *183*, 27; b) E. Donath, S. Moya, B. Neu, G. B. Sukhorukov, R. Georgieva, A. Voigt, H. Baumler, H. Kiesewetter, H. Möhwald, *Chem.-Eur. J.* **2002**, *8*, 5481; c) F. Caruso, *Chem.-Eur. J.* **2000**, *6*, 413.

- [16] a) W. Cho, H. J. Lee, M. Oh, *J. Am. Chem. Soc.* **2008**, *130*, 16943; b) W. J. Rieter, K. M. L. Taylor, H. Y. An, W. L. Lin, W. B. Lin, *J. Am. Chem. Soc.* **2006**, *128*, 9024; c) Z. Ni, R. I. Masel, *J. Am. Chem. Soc.* **2006**, *128*, 12394; d) M. Oh, C. A. Mirkin, *Nature* **2005**, *438*, 651; e) J. Cravillon, R. Nayuk, S. Springer, A. Feldhoff, K. Huber, M. Wiebcke, *Chem. Mater.* **2011**, *23*, 2130; f) N. Yanai, S. Granick, *Angew. Chem., Int. Ed.* **2012**, *51*, 5638; g) N. Yanai, M. Sindoro, J. Yan, S. Granick, *J. Am. Chem. Soc.* **2013**, *135*, 34; h) M. Tsotsalas, A. Umemura, F. Kim, Y. Sakata, J. Reboul, S. Kitagawa, S. Furukawa, *J. Mater. Chem.* **2012**, *22*, 10159.
- [17] S. M. Cohen, *Chem. Rev.* **2012**, *112*, 970.
- [18] K. S. Park, Z. Ni, A. P. Cote, J. Y. Choi, R. D. Huang, F. J. Uribe-Romo, H. K. Chae, M. O'Keeffe, O. M. Yaghi, *Proc. Natl. Acad. Sci. U.S.A.* **2006**, *103*, 10186.
- [19] a) M. Losche, J. Schmitt, G. Decher, W. G. Bouwman, K. Kjaer, *Macromolecules* **1998**, *31*, 8893; b) G. Ladam, P. Schaad, J. C. Voegel, P. Schaaf, G. Decher, F. Cuisinier, *Langmuir* **2000**, *16*, 1249.
- [20] C. Dejognat, G. B. Sukhorukov, *Langmuir* **2004**, *20*, 7265.
- [21] A. A. Antipov, G. B. Sukhorukov, E. Donath, H. Möhwald, *J. Phys. Chem. B* **2001**, *105*, 2281.
- [22] R. Heuberger, G. Sukhorukov, J. Voros, M. Textor, H. Möhwald, *Adv. Funct. Mater.* **2005**, *15*, 357.
- [23] C. Cortez, E. Tomaskovic-Crook, A. P. R. Johnston, A. M. Scott, E. C. Nice, J. K. Heath, F. Caruso, *ACS Nano* **2007**, *1*, 93.
- [24] S. Beyer, J. H. Bai, A. M. Blocki, C. Katak, Q. R. Xue, M. Raghunath, D. Trau, *Soft Matter* **2012**, *8*, 2760.
- [25] K. Haberska, T. Ruzgas, *Bioelectrochemistry* **2009**, *76*, 153.
- [26] U. P. N. Tran, K. K. A. Le, N. T. S. Phan, *ACS Catal.* **2011**, *1*, 120.
- [27] a) Y. Wang, A. S. Angelatos, F. Caruso, *Chem. Mater.* **2008**, *20*, 848; b) K. Ariga, Q. M. Ji, J. P. Hill, A. Vinu, *Soft Matter* **2009**, *5*, 3562; c) K. Ariga, A. Vinu, Y. Yamauchi, Q. M. Ji, J. P. Hill, *Bull. Chem. Soc. Jpn.* **2012**, *85*, 1; d) K. Ariga, Q. M. Ji, J. P. Hill, Y. Bando, M. Aono, *NPG Asia Mater.* **2012**, *4*, e17.
- [28] L. Wang, H. Yu, *Macromolecules* **1988**, *21*, 3498.
- [29] A. Fery, R. Weinkamer, *Polymer* **2007**, *48*, 7221.
- [30] S. Babae, B. H. Jahromi, A. Ajdari, H. Nayeb-Hashemi, A. Vaziri, *Acta Mater.* **2012**, *60*, 2873.
- [31] N. Delorme, M. Dubois, S. Garnier, A. Laschewsky, R. Weinkamer, T. Zemb, A. Fery, *J. Phys. Chem. B* **2006**, *110*, 1752.



**Scheme 1.** Schematic illustration of LbL assembly on MOF crystals followed by MOF dissolution to form faceted polymer microcapsules.

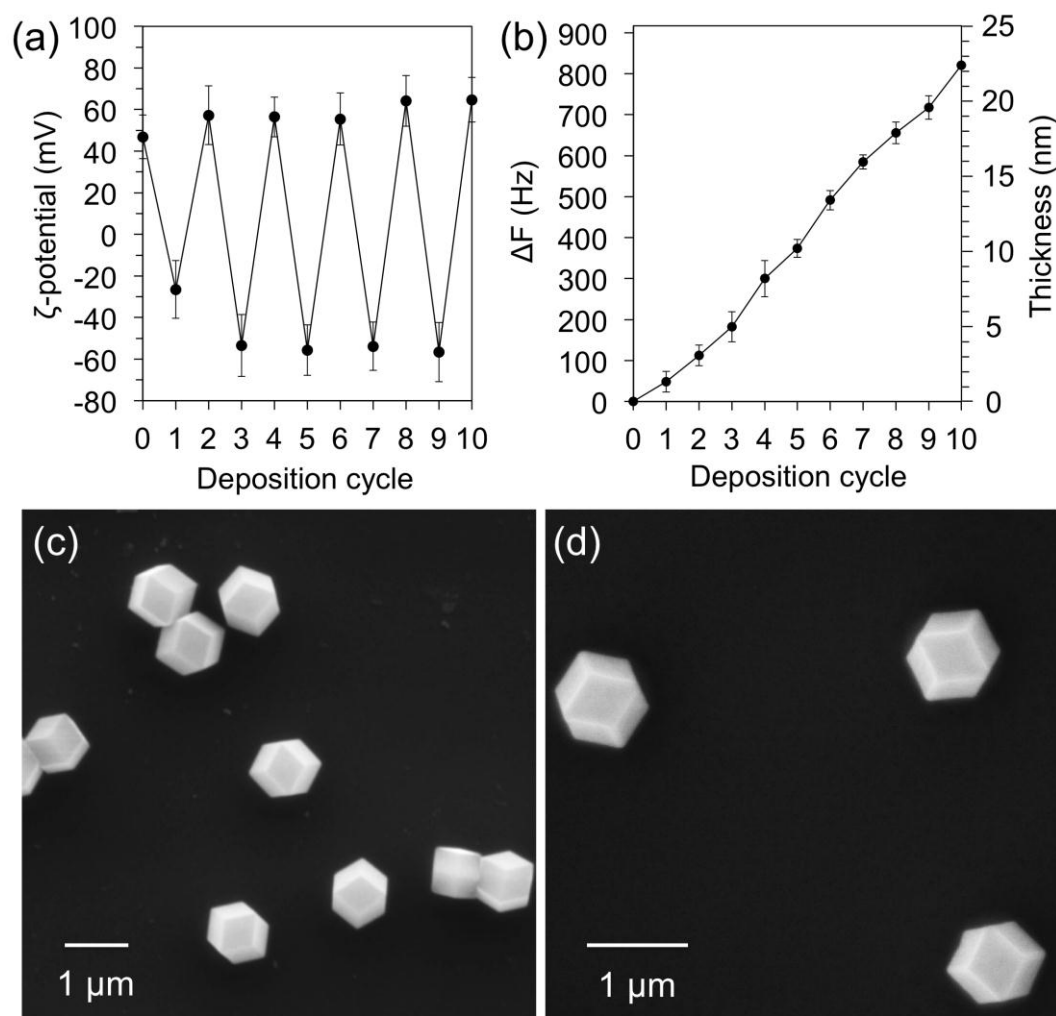


**Figure 1.** LbL coating (PSS/PA) of MOF crystals. (a) Zeta ( $\zeta$ )-potential values plotted against deposition cycle number. (b) Decrease in resonance frequency ( $\Delta F$ ) of QCM resonators plotted against deposition cycle number. Also: SEM images of dry samples before (c), and after (d), the (PSS/PA)<sub>4</sub>/PSS LbL coating.

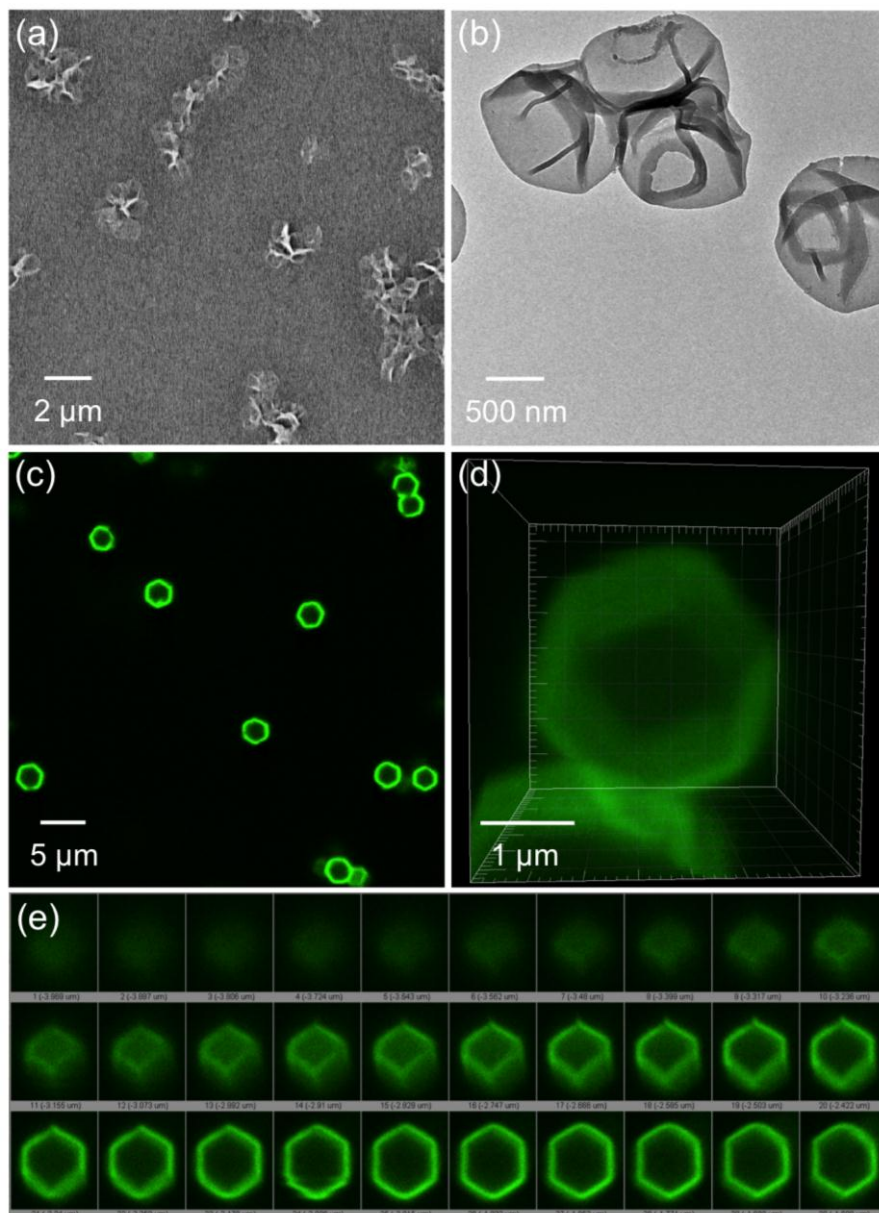


**Figure 2.** Images of faceted polymer capsules obtained using various techniques. (a) SEM, (b) TEM, (c) 2D-CLSM, (d) 3D-CLSM, and (e) CLSM z-slices.

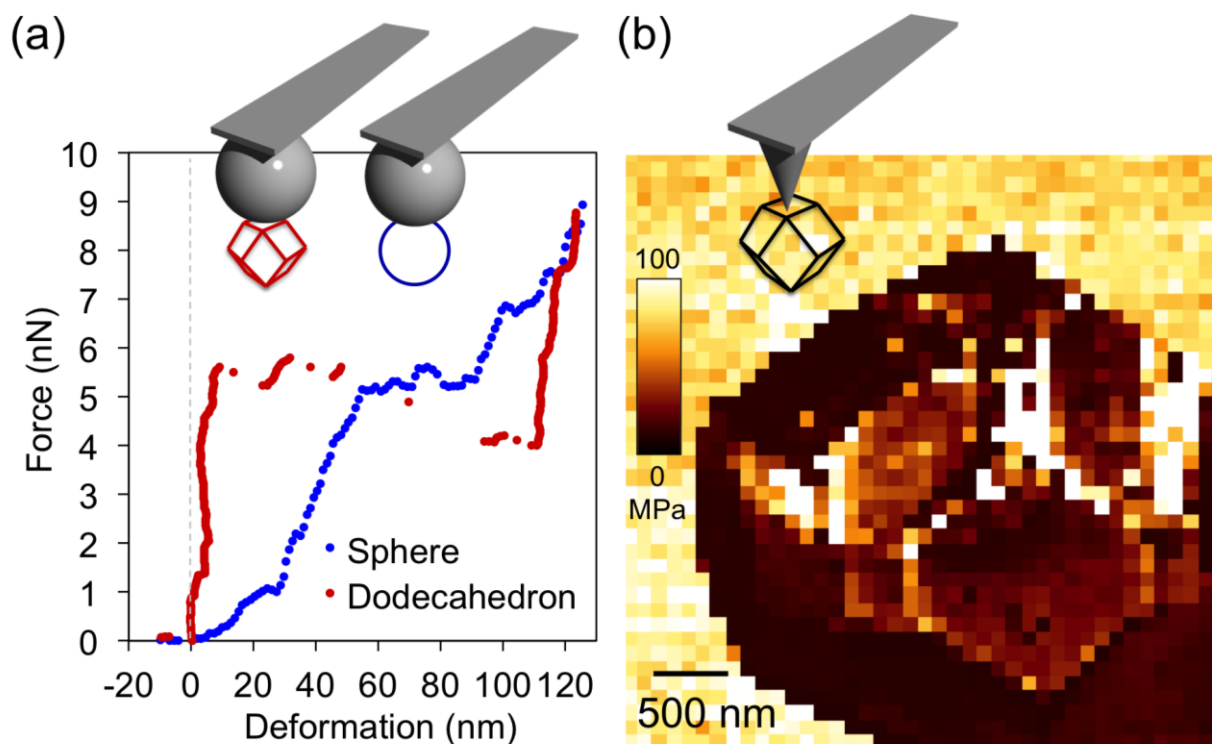


**Figure 3.** Stiffness comparison of the present faceted and conventional spherical capsules, for the same layer thickness and hollow capsule size. (a) Representative colloidal-probe force-deformation curves taken on spherical and rhombic dodecahedral capsules. (b) High resolution 2D force mapping of a rhombic dodecahedral capsule in water.

**Table of contents entry**

Faceted polymer microcapsules are prepared from metal-organic framework (MOF) templates (see figure). The MOF templates are removable under mild aqueous conditions. The obtained microcapsules are stiffer than their spherical counterparts, reflecting the near-incompressibility of the facet edges, and indicating that the faceting might be a useful strategy for controlling the mechanical properties of polymer microcapsules.

Keyword (polymer capsules, metal-organic framework, layer-by-layer, nanomechanics)

H. Ejima, N. Yanai, J. P. Best, M. Sindoro, S. Granick\* and F. Caruso\*

Near-Incompressible Faceted Polymer Microcapsules from Metal-Organic Framework Templates

ToC figure

